



TCN1 Deficiency Inhibits the Malignancy of Colorectal Cancer Cells by Regulating the ITGB4 Pathway

Xinqiang Zhu^{1,2}, Xuotong Jiang², Qinglin Zhang³, Hailong Huang², Xiaohong Shi⁴, Daorong Hou⁵, and Chungeng Xing¹

¹Department of General Surgery, The Second Affiliated Hospital of Soochow University, Suzhou, ²Department of General Surgery, The Affiliated Suqian Hospital of Xuzhou Medical University, Suqian, ³Department of Gastroenterology, Wuxi People's Hospital Affiliated to Nanjing Medical University, Wuxi, ⁴Department of Pathology, The Affiliated Suqian Hospital of Xuzhou Medical University, Suqian, and ⁵Key Laboratory of Model Animal Research, Nanjing Medical University, Nanjing, China

Article Info

Received October 28, 2021

Revised January 21, 2022

Accepted February 10, 2022

Published online June 10, 2022

Corresponding Author

Chungeng Xing

ORCID <https://orcid.org/0000-0001-7865-1258>

E-mail Xingcg@suda.edu.cn

Xinqiang Zhu, Xuotong Jiang, and Qinglin Zhang contributed equally to this work as first authors.

Background/Aims: This study aimed to investigate the biological function and regulatory mechanism of TCN1 in colorectal cancer (CRC).

Methods: We studied the biological function of TCN1 by performing gain-of-function and loss-of-function analyses in HCT116 cell lines; examined the effects of TCN1 on the proliferation, apoptosis, and invasion of CRC cells; and determined potential molecular mechanisms using HCT116 and SW480 CRC lines and mouse xenotransplantation models. Tumor xenograft and colonization assays were performed to detect the tumorigenicity and metastatic foci of cells *in vivo*.

Results: TCN1 knockdown attenuated CRC cell proliferation and invasion and promoted cell apoptosis. Overexpression of TCN1 yielded the opposite effects. In addition, TCN1-knockdown HCT116 cells failed to form metastatic foci in the peritoneum after intravenous injection. Molecular mechanism analyses showed that TCN1 interacted with integrin subunit $\beta 4$ (ITGB4) to positively regulate the expression of ITGB4. TCN1 knockdown promoted the degradation of ITGB4 and increased the instability of ITGB4 and filamin A. Downregulation of ITGB4 at the protein level resulted in the disassociation of the ITGB4/plectin complex, leading to cytoskeletal damage.

Conclusions: TCN1 might play an oncogenic role in CRC by regulating the ITGB4 signaling pathway. (*Gut Liver* 2023;17:412-429)

Key Words: TCN1; Proliferation; Invasion; Colorectal neoplasms; ITGB4 pathway

INTRODUCTION

Colorectal cancer (CRC) is one of the most common intestinal tumors in the world.¹ It is also the fourth leading cause of death and the second leading cause of cancer-related death in the world.² The total number of deaths from CRC will increase by approximately 70% by the year 2035.³ Although the development of surgical resection technology has improved the survival rate of early CRC patients, the long-term prognosis of most CRC patients is still poor, the main reason being recurrence and metastasis.^{4,5} However, the exact mechanism is still unclear. Molecular mapping of CRC (including at the DNA and protein levels) has become increasingly important for identifying prognostic biomarkers and developing new therapeutic strategies.⁶ Therefore,

identifying new key molecules involved in the progression of CRC will help to provide new therapeutic targets.

Transcobalamin 1 (TCN1), also known as vitamin B₁₂ (cobalamin) R binding protein, is one of the three transporters of vitamin B₁₂, which exists in serum and various biological liquids.⁷ Vitamin B₁₂ plays an important role in hematopoiesis, cell metabolism, and nervous system function.^{8,9} TCN1 carries vitamin B₁₂ through the stomach and is released by enzymes in the duodenum, where it binds to intrinsic factors.^{10,11} Unexpectedly, the overexpression of TCN1 in tumor tissues is associated with tumorigenesis.¹² TCN1 is overexpressed in malignant tumors, such as hepatocellular carcinoma, leukemia, breast cancer, lung cancer, and gastric cancer.^{10,11,13} Bioinformatics-based studies have shown that TCN1 is an important oncogene.¹⁴ Next-

Copyright © Gut and Liver.



This is an Open Access article distributed under the terms of the Creative Commons Attribution Non-Commercial License (<http://creativecommons.org/licenses/by-nc/4.0>) which permits unrestricted non-commercial use, distribution, and reproduction in any medium, provided the original work is properly cited.

generation sequencing confirmed that TCN1 is one of the overexpressed genes in CRC.¹⁵ Previously, Liu *et al.* and us also showed that TCN1 expression in CRC was significantly associated with malignant biological behavior.^{16,17} Consequently, it is suggested that TCN1 is related to the occurrence and development of CRC, which is worthy of further study.

Integrin subunit $\beta 4$ (ITGB4) is one of the most characteristic integrins and is involved in regulating a variety of cell functions.¹⁸ Integrins affect the migration, invasion, proliferation, and survival of tumor cells and regulate the angiogenesis, connective tissue proliferation, and immune response of tumor host cells, thereby affecting epithelial-mesenchymal transition (EMT), cancer development, metastasis, and even treatment results.^{19,20} It has been reported that high expression of ITGB4 promotes the occurrence, metastasis, and poor prognosis of different types of tumors.^{21,22} The overexpression of ITGB4 is also associated with aggressive behavior and poor prognosis in breast cancer, bladder cancer, cervical cancer, head and neck cancer, lung cancer, and pancreatic cancer.^{23,24} In this study, we demonstrated that TCN1 and ITGB4 were highly expressed in clinical colorectal tumor samples, and the expression levels were positively correlated; TCN1 deficiency in CRC cells inhibits their growth, adhesion, and invasion by interacting with ITGB4; TCN1 deficiency promotes ITGB4 degradation, facilitates the degradation of ITGB4 and plectin (PLEC), and impairs the stability of filamin A (FLNA) and F-actin networks, and eventually leads to cytoskeleton damage of CRC cells.

MATERIALS AND METHODS

1. Cell culture

The human cell lines (including HCT116, SW480, HCoEpiC, and HEK293T) originated from the American Type Culture Collection (Manassas, VA, USA) and were cultured in RPMI 1640 medium with 10% fetal bovine serum and 1% (v/v) penicillin/streptomycin in a humidified atmosphere of 5% CO₂ at 37°C.

2. Clinical samples

CRC specimens were collected with informed consent from 80 cases of surgical patients in the Affiliated Suqian Hospital of Xuzhou Medical University and Jiangning Hospital Affiliated to Nanjing Medical University between 2011 and 2014 following the protocols approved by the Ethics Committee of the Affiliated Suqian Hospital of Xuzhou Medical University (approval number: 2002014). The samples had paired samples of adjacent normal CRC tis-

sue. The definitive histological diagnosis of each CRC patient was confirmed after surgery, and no patients received radiotherapy or chemotherapy. All participants signed informed consent forms.

3. Immunohistochemistry analysis

Paraffin-embedded tumor tissues or peritumor tissues were cut into 4- μ m-thick sections. The slide was heated by microwave in 0.01 M citrate buffer (pH=6.0) for 10 minutes to recover the antigen. Subsequently, the sections were incubated with primary antibodies (anti-TCN1 rabbit antibody [ab202121, Abcam, Cambridge, UK], anti-ITGB4 rabbit antibody [ab182120, Abcam], anti-Ki-67 antibody [ab16667, Abcam], and anti-PCNA antibody [ab92552, Abcam]) in a humidified chamber overnight at 4°C. Horseradish peroxidase-labeled secondary antibodies were incubated at room temperature for 1 hour. All CRC sections were examined by two experienced pathologists. TCN1 or ITGB4 staining was independently scored by two pathologists who did not know the clinical data using the H-score system.²⁵ The intensity of immunostaining was 0–3: 0, negative; 1, weak; 2, medium; 3, strong. H score was the product of different staining intensities in 0–3 and the percentage of positive cells.

4. Quantitative polymerase chain reaction

Total RNA was extracted from snap-frozen CRC tumor tissues and paired noncancerous tissues using TRIzol Reagent (B5704-1; Takara, Kusatsu, Japan), followed by treatment with DNase I (2212, Takara). After the RNA concentration was determined by spectrophotometer (NanoDrop 2000c; Thermo Scientific, Waltham, MA, USA), the cDNA was synthesized using PrimeScriptTM RT reagent Kit (RR037A, Takara). Quantitative polymerase chain reaction (Q-PCR) was performed using the LightCycler PCR QC Kit (6746381001; Roche Basel, Switzerland) and a 7300 Real-Time PCR System (LC96, Roche). Human TCN1- and GAPDH-specific primers listed in Supplementary Table 1. The relative expression level of the target genes was normalized to that of the GAPDH and calculated by the Δ Ct method (Δ Ct=[mean Ct–mean Ct GAPDH]).²⁶ Data analysis was performed using GraphPad Prism 8 software (GraphPad Software, San Diego, CA, USA).

5. Survival analysis

Survival analysis was performed on 80 patients, and the survival curves were drawn according to the Kaplan-Meier method. Patients were divided into TCN1 and ITGB4 high expression group (Δ Ct \leq 4.25) and low expression group (Δ Ct $>$ 4.25) according to the median levels of TCN1 and ITGB4 in cancer tissues. Overall survival was the time

from surgery to patient's death. Follow-up was for 60 months, although patients who survived beyond 5 years were still followed up.

6. Generation of stable cell lines using lentivirus infection

To generate a lentivirus expressing short hairpin RNA targeting human TCN1 (GenBank Accession No. NM_001062.4), the shTCN1 sequences listed in Supplementary Table 1 were designed and synthesized. HEK293T cells were co-transfected with lentiviral expression constructs (4 μ g), viral envelope plasmid (pMD2.G, 4 μ g), and viral packaging plasmid (psPAX2, 4 μ g) using Lipofectamine 2000 (Invitrogen, Waltham, MA, USA). The empty vector was used as a short hairpin RNA control (TCN1-KDC). The expression constructs (TCN1-KD1, TCN1-KD2, and TCN1-KDC) plasmid maps are listed in Supplementary Fig. 1A and B. After 72 hours of transfection, the virus supernatant was collected and purified by 0.45 μ m filters. The mCherry-expressing lentiviruses, including LV-TCN1-KD1, LV-TCN1-KD2, and LV-TCN1-KDC, were then concentrated by ultracentrifugation (20,000 rpm) for 2 hours.

The full-length coding sequence of human TCN1 was cloned into pLenti-CMV-Puro-mCherry lentiviral plasmid (CAVR Gene, Zhenjiang, China) to construct the recombinant TCN1-overexpression lentivirus (TCN1-OE). The empty vector was used as a short hairpin RNA control (TCN1-OEC). HCT116 and SW480 cells were infected with LV-TCN1-KD1, LV-TCN1-KD2, LV-TCN1-KDC, LV-TCN1-OE and LV-TCN1-OE plus 8 μ g/mL polybrene. Twenty-four hours after lentiviral infection, the cells were selected using puromycin (2 μ g/mL; Sigma-Aldrich, St. Louis, MO, USA) prior to use in experiments. The primer sequences for TCN1 cloning are listed in Supplementary Table 1. The TCN1-OE plasmid maps are listed in Supplementary Fig. 1C and D.

7. Cell apoptosis and proliferation detection

The apoptosis and proliferation rate of HCT116 cells were detected using annexin V fluorescein isothiocyanate (FITC) detection kit (556547; BD Biosciences, Franklin Lake, NJ, USA) and cell light EdU Apollo 488 in vitro Kit (C10310-3; Ribobio, Guangzhou, China) according to the manufacturer's instruction. Samples were analyzed using flow cytometry (BD FACSCalibur, BD Biosciences).

8. Cell invasion assay

Briefly, cells were seeded in insert plates with Matrigel (BD Biosciences) coating and 24 well tissue culture plates. After 24 hours of culture, the cells migrated below the insert plate were stained with 0.4% crystal violet and photo-

graphed (IX-71; Olympus, Tokyo, Japan).

9. Cell viability

Cell viability was detected at 0, 12, 24, 36, 48, and 60 hours using Cell Counting Kit-8 (CCK-8) reagent (HY-K0301; MedChemExpress, Monmouth Junction, NJ, USA). Briefly, the cells were washed twice with phosphate buffered saline (PBS). Then, 100 μ L RPMI 1640 medium and 10 μ L CCK-8 solution were added to each well. The cells were incubated for 1.5 hours at 37°C, and the absorption value was detected at 450 nm. All experiments were repeated three times.

10. Immunofluorescence staining

HCT116 cells were fixed with 4% formaldehyde for 15 minutes at room temperature. After washing the cells 3 times in PBS with 0.1% Triton X-100, cells were blocked with 4% bovine serum albumin for 30 minutes. Cells were incubated with primary ITGB4 antibody (ab182858, Abcam), ITGA3 (ab131055, Abcam), FLNA antibody (4762; Cell Signaling Technology, Danvers, MA, USA), FITC-phalloidin antibody (P5282, Sigma) and PLEC antibody (ab11220, Abcam) for 1 hour at room temperature. Following washes with PBS, 0.1% Triton X-100, cells were incubated with FITC/TRITC-conjugated secondary antibodies for 1 hour at room temperature. Following washes with PBS, 0.1% Triton X-100, cells were stained with DAPI (Sigma) and visualized by confocal scanning microscopy (710; Zeiss, Oberkochen, Germany). The original TIF images were quantified by immunofluorescence using ImageJ software (National Institutes of Health, Bethesda, MD, USA). Signal and background intensity was measured. The net fluorescence intensity is obtained by subtracting the background intensity from the signal intensity.

11. Transmission electron microscopy assays

The cells were fixed in 2.5% glutaraldehyde (pH 7.4) at 4°C for 48 hours, and then in 0.5% osmium tetroxide for 24 hours. After dehydration, the samples were embedded in epoxy resin to make ultrathin sections (70-nm-thick) and examined by transmission electron microscope (Tecnai G2 Spirit Bio TWIN; FEI Co., Hillsboro, OR, USA).

12. RNA-sequence analysis

Total RNA was extracted from TCN1-KD1, TCN1-KD2, TCN1-KDC, TCN1-OE and TCN1-OEC HCT116 cell lines. RNA degradation and contamination were monitored on 1% agarose gels. RNA purity was checked using the NanoPhotometer spectrophotometer (Implen, Westlake Village, CA, USA). RNA concentration was measured using Qubit RNA Assay Kit in Qubit 2.0 Fluorometer (Life

Technologies, CA, USA). RNA integrity was assessed using the RNA Nano 6000 Assay Kit of the Agilent Bioanalyzer 2100 system (Agilent Technologies, Westlake Village, CA, USA). A total amount of 2 µg RNA per sample was used as input material for the RNA sample preparations. PCR products were purified (AMPure XP system) and library quality was assessed on the Agilent Bioanalyzer 2100 system. After cluster generation, the library preparations were sequenced on an Illumina HiSeq 4000 platform and paired-end 150 bp reads were generated. The genes with a fold change value greater than 2, and a p-value <0.01 were considered differentially expressed. Relationships of differentially expressed genes were determined by Gene Ontology analysis and gene set enrichment analysis (GSEA).

13. Chromatin immunoprecipitation assays

Chromatin immunoprecipitation assays were performed as described previously.²⁷ The protein–DNA complexes were immunoprecipitated using anti-TCN1 antibody (ab202121, Abcam), anti-ITGB4 antibody (ab182120, Abcam) or immunoglobulin G (IgG; ab172730, Abcam), which served as a control. Chromatin immunoprecipitation samples were analyzed by quantitative real-time PCR. The primer sequences for Chips are listed in Supplementary Table 1.

14. Establishment of tumor xenografts in nude mice

All animal experimental procedures were approved by the Animal Care and Use Committee of Nanjing Medical University (approval number: IACUC-2002014). The tumor xenografts were established in nude mice by subcutaneous implantation. mCherry-labeled HCT116 cells in logarithmic phase were digested with trypsin, rinsed three times with 1× PBS, and then suspended in 100 µL of 1× PBS. Thirty BALB/c nude mice (4 weeks old, male) were randomly divided into five groups (TCN1-KDC, TCN1-KD1, TCN1-KD2, TCN1-OEC, and TCN1-OE) and housed at 22°C on a 12/12-hour light/dark cycle and freely received standard mouse chow and tap water. A total of 2.5×10^6 cells were inoculated into the inner fat pad at the root of right leg of mice. Tumor growth was measured and quantified weekly using bioluminescence imaging (IVIS Spectrum; PerkinElmer, Waltham, MA, USA). The growth of the primary tumor was also monitored with a caliper every week for 6 weeks. The tumor volume was calculated using the formula: $0.5 \times \text{length} \times \text{width}^2$. The tumors were collected after mice were sacrificed under general anesthesia using intraperitoneal injection of pentobarbital sodium (150 mg/kg).

15. Colonization assay in nude mice

HCT116 cells (1×10^6 cells/mouse) were injected into BALB/c nude mice (n=6) through tail vein. At 60 days after inoculation, the metastatic foci in mice were measured and quantified using bioluminescence imaging (IVIS Spectrum, PerkinElmer). The intestines were collected for fluorescence quantification and fixed in 4% paraformaldehyde after mice were sacrificed under general anesthesia using intraperitoneal injection of pentobarbital sodium (150 mg/kg). Metastatic nodules were immunohistochemically stained with anti-TCN1 rabbit antibody (ab202121, Abcam), anti-ITGB4 rabbit antibody (ab182120, Abcam). Tissue staining was detected under a light microscope (1-71, Olympus), and protein expression was quantified using ImageJ software (National Institutes of Health).

16. Western blot analysis

The cells and cancer tissues were lysed in RIPA lysis buffer containing 1 mM phenylmethylsulfonyl fluoride (Biotek Co., Wuxi, China). Protein samples (50 µg) were separated on a 10% SDS-PAGE gel and transferred to nitrocellulose membranes. TBST buffer (100 mM NaCl, 10 mM Tris HCl, and 0.1% Tween 20) containing 5% skim milk was used to block the membrane at room temperature for 1 hour. Then, the membrane was incubated with primary antibodies against TCN1 (ab202121, Abcam), ITGB4 (ab182120, Abcam), FLNA (4762, Cell Signaling Technology) and GAPDH (sc-166574; Santa Cruz Biotechnology, Inc., Santa Cruz, CA, USA) at 4°C overnight. On the second day, a horseradish peroxidase-conjugated goat anti-rabbit IgG secondary antibody (sc-2004, Santa Cruz Biotechnology, Inc.) or goat anti-mouse IgG horseradish peroxidase binding secondary antibody (sc-2005, Santa Cruz Biotechnology, Inc.) was incubated with the membrane for 1 hour at room temperature. Then, the membrane was rinsed three times with TBST. Western blot analyses were performed with Pierce ECL Western Blotting Substrate (32209; Thermo Fisher Scientific, Waltham, MA, USA) and a ChemiDoc XRS⁺ molecular imager (Bio-Rad, Hercules, CA, USA), and quantitative analysis was performed with ImageJ software (National Institutes of Health).

17. Statistical analysis

Data are presented as the mean±standard deviation. Statistical analyses were performed using GraphPad 8.0 statistical software (GraphPad Software). One way analysis of variance was used to compare the differences among the groups. Statistically significant differences were examined using two-tailed Student t-test, two-sided Pearson chi-square test, or the log-rank (Mantel-Cox) test to derive the

significance of the differences between two groups. $p < 0.05$ was considered to be significant.

RESULTS

1. TCN1 is overexpressed in CRC tissues and positively correlates with poor prognosis of CRC patients

To investigate the clinical significance of TCN1 and

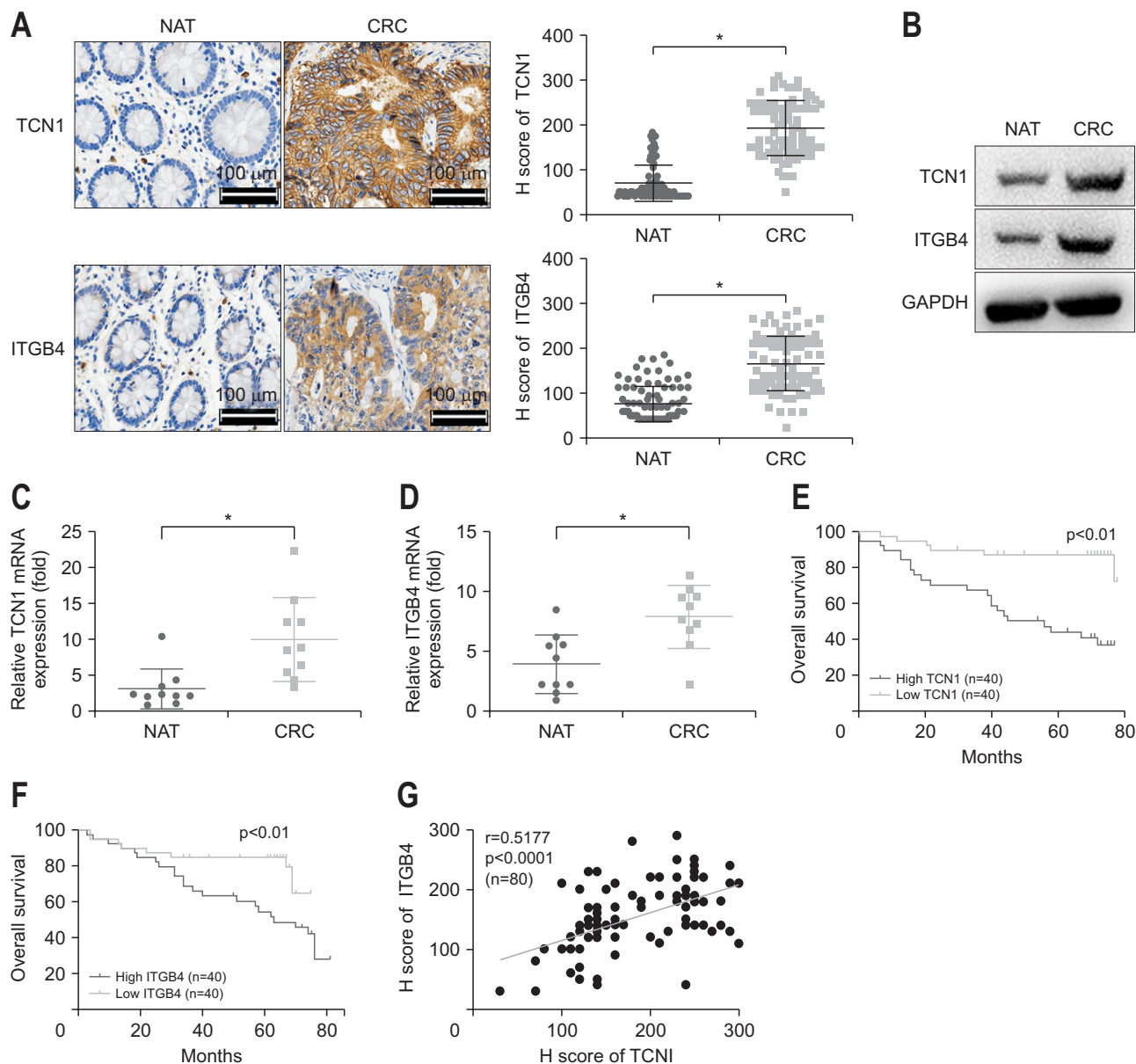


Fig. 1. Transcobalamin 1 (TCN1) and integrin subunit B4 (ITGB4) are highly expressed in colorectal cancer (CRC) clinical tissues. (A) Immunohistochemistry analysis of TCN1 and ITGB4 in CRC tissue. Representative pictures of immunohistochemical staining are shown (n=80). (B) Western blot analysis of TCN1 and ITGB4 in CRC tissue specimens (n=6). Representative pictures of Western blot analysis of TCN1 and ITGB4 in six pairs of CRC tissues and adjacent nontumor normal tissues (NATs) from six CRC cases are shown. (C, D) Real-time quantitative polymerase chain reaction (PCR) analysis of TCN1 and ITGB4. RNA samples were extracted from 80 pairs of CRC tissues and normal tissues for real-time quantitative PCR analysis of TCN1 and ITGB4 expression (n=10). The levels of TCN1 and ITGB4 mRNA were expressed as $\Delta Ct = (\text{mean } Ct \text{ target} - \text{mean } Ct \text{ GAPDH})$. $p < 0.01$ compared with NAT tissue. (E) Kaplan-Meier survival curves for CRC patients grouped according to the median expression level of TCN1 indicated that patients with high TCN1 expression had a shorter overall survival time after surgery (n=40). (F) Kaplan-Meier survival curves for CRC patients grouped according to the median expression level of ITGB4 indicated that patients with high ITGB4 expression had a shorter overall survival time after surgery (n=40). (G) Pearson correlation scatter plot of TCN1 and ITGB4 H scores in human CRC tissue (n=80). All experimental data are presented as the mean \pm SD. Statistical significance, * $p < 0.01$.

ITGB4 expression in CRC patients, we detected the protein expression of TCN1 and ITGB4 in CRC specimens and adjacent tissues. Immunohistochemistry and Western blot analysis showed significant upregulation of TCN1 and ITGB4 expression in human CRC tissues compared to normal tissues ($p < 0.01$) (Fig. 1A and B). Next, we analyzed TCN1 and ITGB4 mRNA expression in CRC specimens. We found that the transcription levels of TCN1 and ITGB4 were significantly higher in CRC tissues than in paired peritumor tissues (Fig. 1C and D). The Kaplan-Meier survival analysis showed that patients with high expression of TCN1 and ITGB4 had shorter overall survival than other CRC patients (Fig. 1E and F). Notably, the expression of TCN1 and ITGB4 correlated well across all CRC samples analyzed (Fig. 1G). In addition, the expression of TCN1 was significantly correlated with clinicopathological variables such as TNM stage, G3 stage, depth of tumor invasion and serum carcinoembryonic antigen level (including regional lymph node metastasis and tumor size), while the expression of TCN1 was not correlated with age, gender, tumor location or nerve invasion (Table 1). These results indicated that high TCN1 expression was associated with high ITGB4 expression, poor prognosis and malignancy of CRC, suggesting that TCN1 may promote CRC progression in conjunction with ITGB4.

2. Lentivirus-mediated TCN1 knockdown and overexpression in CRC cells

We analyzed lentivirus-mediated TCN1-knockdown or overexpression in HCT116 and SW480 cells using Q-PCR and Western blot (Fig. 2A and B). We found that the expression of TCN1 and ITGB4 in TCN1-knockdown (TCN1-KD) cells was reduced to 20% and 25% of the negative control (TCN1-KDC) cells, and TCN1 expression in cells with TCN1 overexpression (TCN1-OE cells) was about 10 times higher than that in cells transfected with the scrambled negative control (TCN1-OEC cells) (Fig. 2A). The protein levels of TCN1 were confirmed by Western blot analysis (Fig. 2B). Our results confirmed the successful generation of lentivirus-mediated TCN1-silenced HCT116 and SW480 cell lines (TCN1-KD1 and TCN1-KD2) and a TCN1-overexpressing CRC cell lines (TCN1-OE) (Supplementary Fig. 1E). The effects of TCN1 on apoptosis were assessed by flow cytometric analysis (Fig. 2C). Annexin V/PI staining revealed that apoptosis in TCN1-KD1 and TCN1-KD2 groups was significantly increased compared with that in TCN1-KDC groups in HCT116 and SW480 cells ($p < 0.01$). Moreover, transwell assays showed the invasion ability of HCT116 and SW480 cells was also significantly decreased in TCN1-KD1 and TCN1-KD2 cells compared with TCN1-KDC cells ($p < 0.01$)

Table 1. Relationship between TCN1 Immunorexpression and Clinicopathological Characteristics in Patients with Colorectal Cancer

Parameter	TCN1 expression level		p-value
	Low	Strong	
Age			0.735
≥65 yr	9	19	
<65 yr	31	21	
Sex			0.746
Female	22	18	
Male	18	22	
CEA level			0.003
Increased	9	24	
Normal	31	16	
CA125 level			0.152
Increased	0	10	
Normal	40	30	
CA19-9 level			0.113
Increased	4	12	
Normal	36	28	
TNM stage			0.065
I-II	29	19	
III-IV	11	21	
Tumor location			0.128
Colon	4	16	
Distal colon	15	6	
Rectum	21	18	
Histological differentiation			
G1	13	4	0.063
G2	23	16	0.085
G3	4	20	0.017
Depth of invasion			
T1/T2	23	2	0.005
T3/T4	17	38	0.003
Tumor size			
≤5 cm	31	14	0.011
>5 cm	9	26	0.018
Metastases to regional lymph nodes			<0.001
No	40	9	
Yes	0	31	
Nerve invasion			0.439
No	32	24	
Yes	8	16	

TCN1, transcobalamin 1; CEA, carcinoembryonic antigen; CA125, cancer antigen 125; CA19-9, cancer antigen 19-9.

and were markedly increased in TCN1-OE cells compared with TCN1-OEC cells ($p < 0.05$) (Fig. 2D and E). The effect of TCN1 on human CRC cell proliferation was assessed by EdU and CCK-8 assay (Fig. 2F-K). The EdU positive cells were significant decrease in TCN1-KD1 and TCN1-KD2 cells compared with TCN1-KDC cells ($p < 0.01$ or $p < 0.05$) (Fig. 2F, G, I, and J), and the EdU positive cells of TCN1-OE cells was markedly increased compared with that of TCN1-OEC cells ($p < 0.01$ or $p < 0.05$). As shown in Fig. 2H and K, a significant decrease in cell viability was detected in TCN1-KD1 and TCN1-KD2 cells compared with TCN1-KDC cells at each time point ($p < 0.01$). In contrast, the viability of TCN1-OE cells was markedly increased

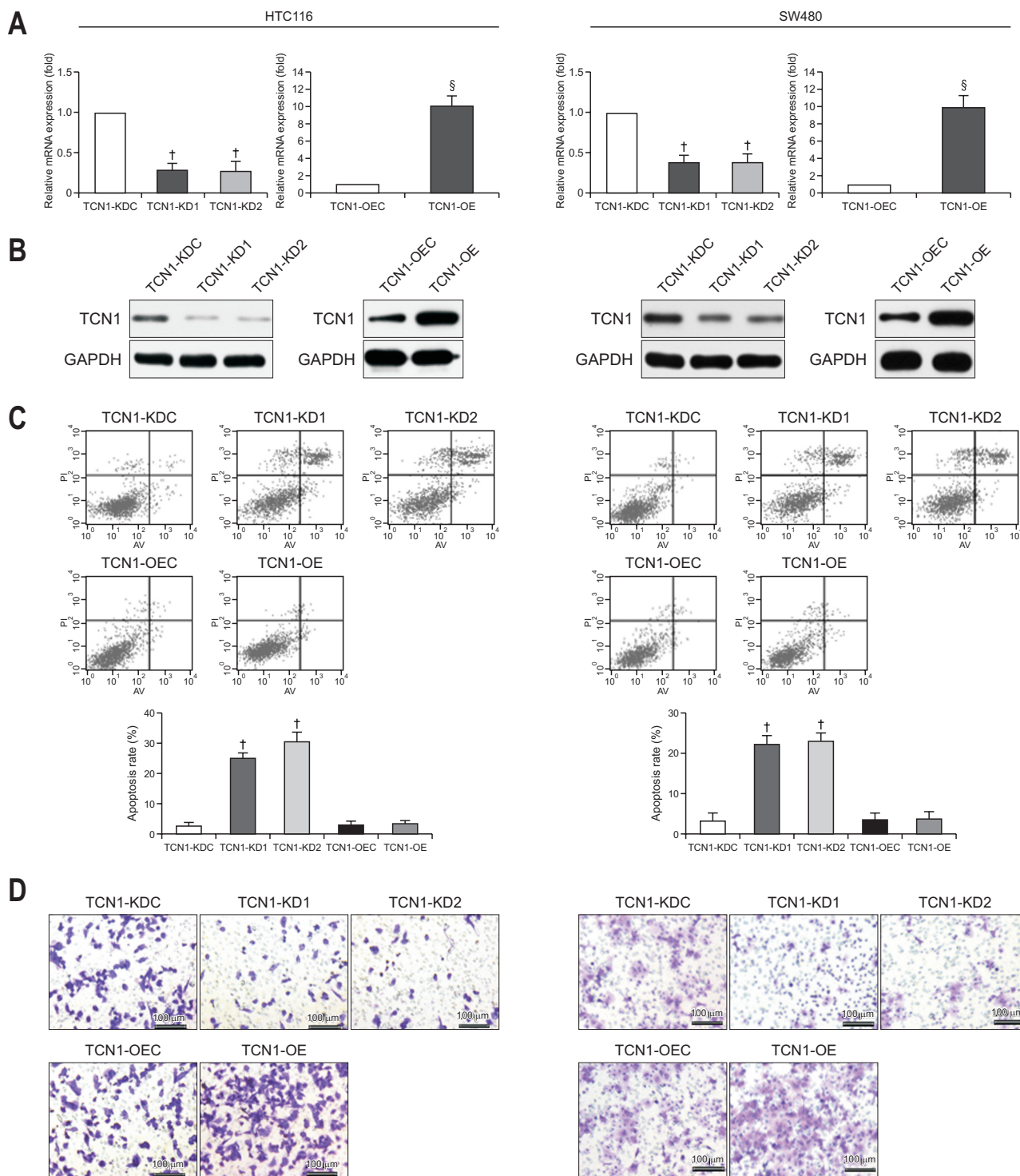


Fig. 2. Lentivirus-mediated knockdown (KD) and overexpression (OE) of transcobalamin 1 (TCN1) in HCT116 cells. (A, B) Expression of TCN1 in TCN1-KD and TCN1-OE HCT116 and SW480 cells assessed by quantitative polymerase chain reaction and Western blot (n=6). (C) Cell apoptosis was detected in TCN1-KD and TCN1-OE HCT116 and SW480 cells using flow cytometry, as indicated (n=6). (D, E) Transwell invasion assays were conducted with TCN1-KD and TCN1-OE HCT116 and SW480 cells, as indicated (n=6). The numbers of invaded cells are displayed in quantitative bar graphs. (F, G) The proliferation of cells was measured by flow cytometry after HCT116 cells were stained with Apollo 488 fluorescence dye to label EdU. (H, I) Proliferation of HCT116 cells at 0, 12, 24, 36, 48, and 60 hours after TCN1-KD and TCN1-OE (n=6). (J, K) The proliferation of cells was measured by flow cytometry after SW480 cells were stained with Apollo 488 fluorescence dye to label EdU. (L, M) Proliferation of SW480 cells at 0, 12, 24, 36, 48, and 60 hours following TCN1-KD and TCN1-OE (n=6). All experimental data are presented as the mean±SD of 3 independent experiments. Statistical significance: compared with TCN1-KDC cells, *p<0.05 and †p<0.01; compared with TCN1-OEC cells, ‡p<0.05 and §p<0.01.

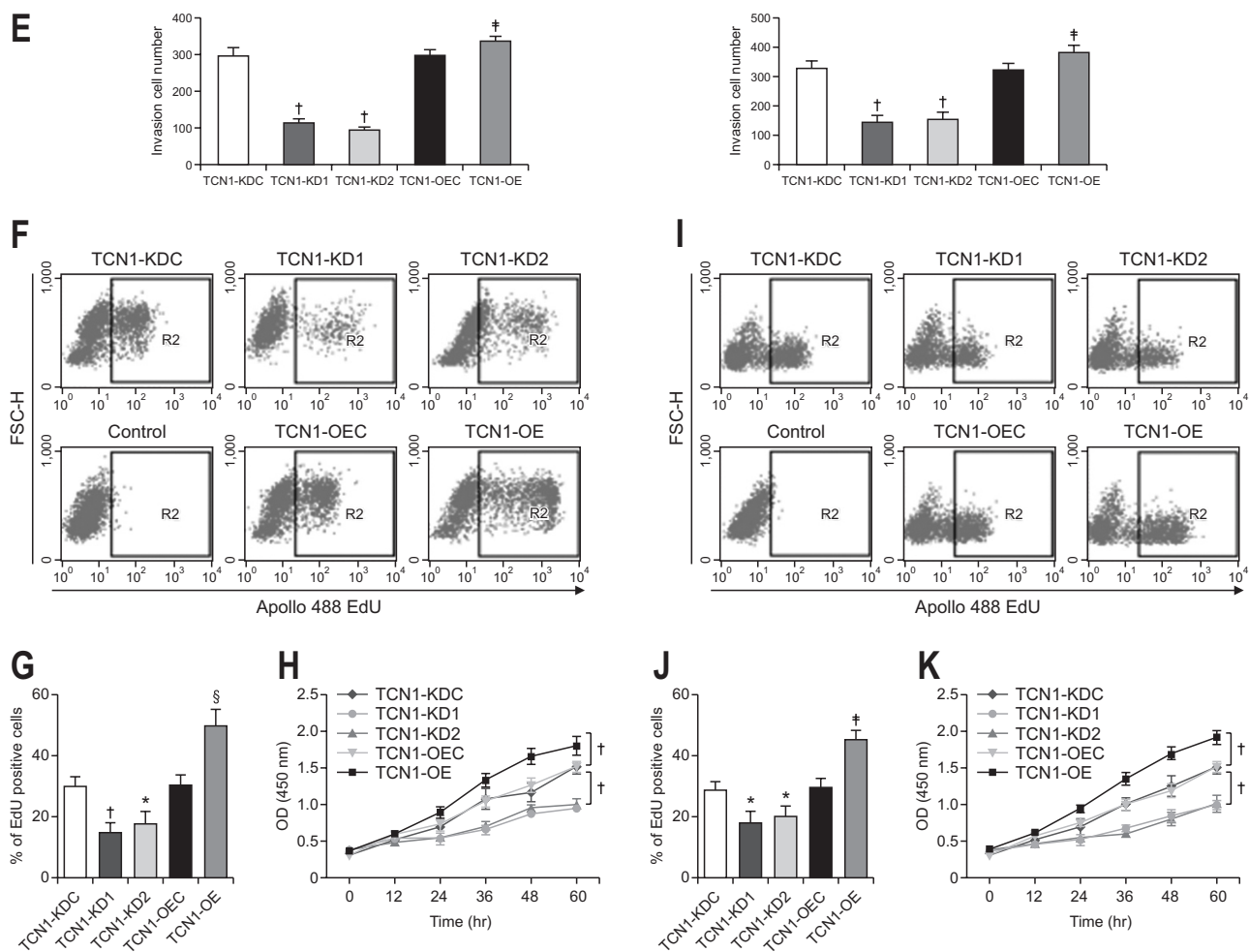


Fig. 2. Continued.

compared with that of TCN1-OEC cells ($p < 0.01$). The data indicated that knockdown of TCN1 inhibits CRC cell proliferation *in vitro*.

3. ITGB4 is a direct downstream transcriptional target of TCN1 in CRC cells

The results above indicated that TCN1 can promote the proliferation of CRC cells. To identify their potential downstream targets and understand their mechanism of action, we performed RNA-sequence assay using mRNA from cells of TCN1-KD1, TCN1-KD2, TCN1-KDC, TCN1-OE, and TCN1-OEC (Fig. 3A). GSEA showed that cell proliferation, cell migration, and Wnt signaling gene were enriched in TCN1-KD1 and TCN1-KD2 cells compared to the control (Supplementary Fig. 2). Consistently, Gene Ontology analysis of differentially expressed genes in TCN1 knockdown cells and control cells showed that several key cellular processes related to cancer progression, such as Wnt signaling, Notch signaling, cell division, cell migration, and proliferation, were significantly enriched

(Fig. 3B).

From gene profile data, we found a total of 77 down-regulated genes in TCN1-KD1 and 156 down-regulated genes in TCN1-KD2 versus negative control with at least a 2-fold change, whereas there were 41 up-regulated genes in TCN1-OE versus controls with at least a 2-fold change. There were 11 common genes which exhibited at least 2-fold downregulation in all knockdown and 2-fold up-regulation in all overexpression profiles (Fig. 3C). Since ITGB4 is a key factor in the Notch signaling pathway, the expression of TCN1 and ITGB4 was consistent in clinical samples, and genes transcriptional analysis showed that ITGB4 was among the 11 overlapping gene list (Fig. 3C), we chose ITGB4 for further investigation as potential downstream target gene of TCN1. We analyzed ITGB4-antibody immune-precipitate from HCT116 cells by immunoblot and found that ITGB4 co-immunoprecipitated with TCN1, the overlap between TCN1 and ITGB4 proteins was verified (Fig. 3D). We also performed chromatin immunoprecipitation analysis using anti-TCN1 antibodies

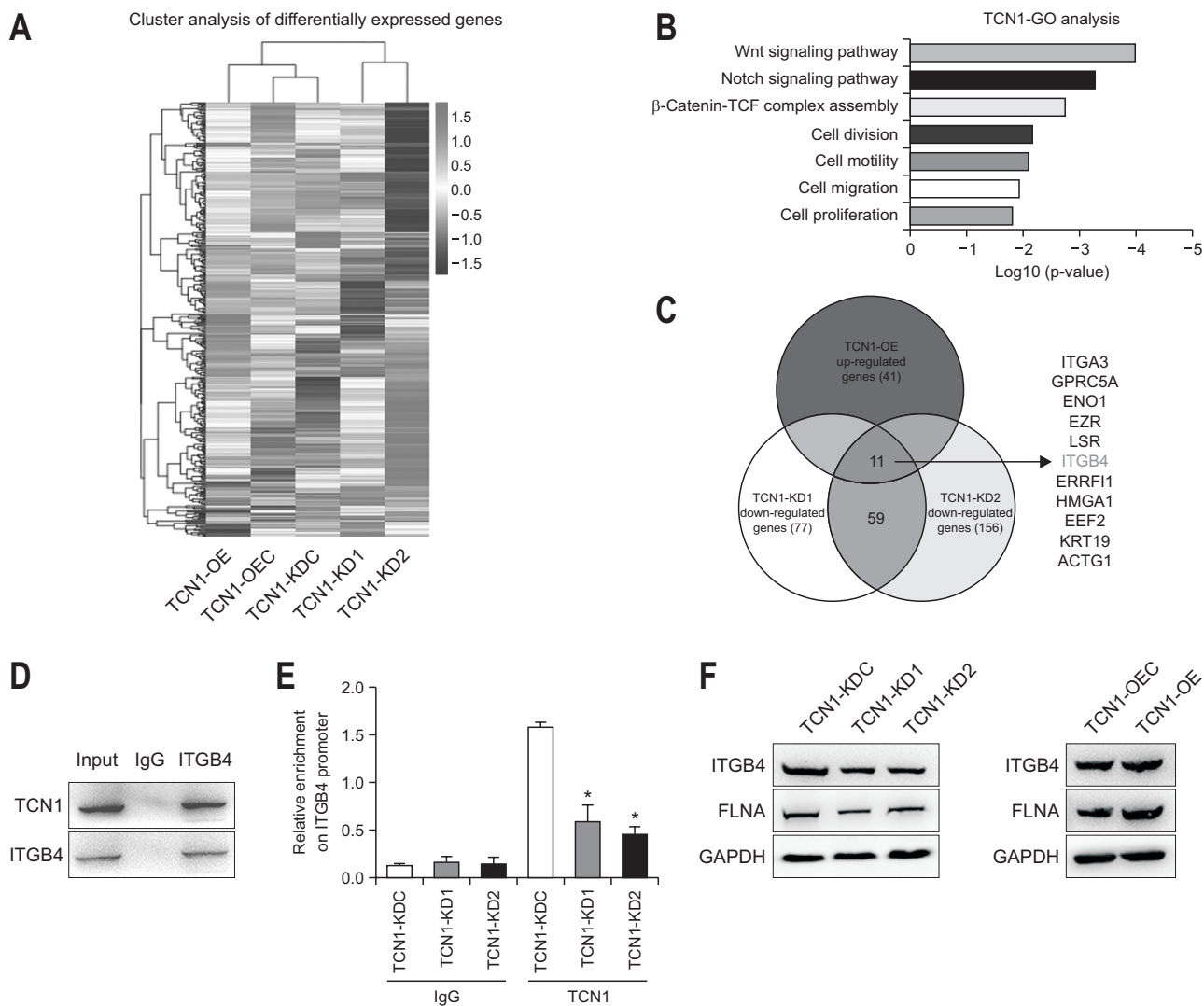


Fig. 3. Integrin subunit B4 (ITGB4) is a direct downstream transcriptional target of transcobalamin 1 (TCN1) in HCT116 cells. (A) Heatmap showing differential mRNA expression in TCN1-KD and TCN1-OE cells (fold change value >1.5 and $p < 0.01$), as indicated. (B) Gene Ontology (GO) analysis of the target genes of TCN1 arranged into functional groups. (C) Venn diagram illustrating the overlap of target genes identified by microarray analysis as being regulated by TCN1 and ITGB4 in HCT116 cells. (D) An interaction between TCN1 and ITGB4 was detected in the coimmunoprecipitation analysis in normal HCT116 cells using anti-ITGB4 antibodies. (E) Chromatin immunoprecipitation analysis of TCN1 binding to the ITGB4 promoter in TCN1-KDC and TCN1-KD HCT116 cells (n=6). (F) Expression of ITGB4 and FLNA in TCN1-knockdown and TCN1-overexpressing HCT116 cells assessed by Western blot analysis (n=6). GAPDH served as the loading control. All experimental data are presented as the mean \pm SD. TCN1-KD, TCN1-knockdown, TCN1-OE, TCN1-overexpression. *Statistical significance: $p < 0.01$.

on the promoter of ITGB4 to determine whether TCN1 directly regulates ITGB4 transcription. The results showed that knockdown of TCN1 led to a significant reduction in TCN1 enrichment on the promoter of ITGB4 in HCT116 cells ($p < 0.01$) (Fig. 3E), suggesting that TCN1 bound to the promoter and directly regulated the transcription of ITGB4. In addition, knockdown of TCN1 in HCT116 cells led to significantly decreased expression of ITGB4 and FLNA, and overexpression of TCN1 in HCT116 cells results in markedly increased expression of ITGB4 and FLNA at the protein levels (Fig. 3F).

4. TCN1 deficiency causes cytoskeletal network damage

The binding of integrin to the cytoskeleton is essential for the stable adhesion of integrin to the extracellular matrix (ECM).²⁸ PLEC and ITGB4 are hemidesmosomes, which play an important role in maintaining the integrity of the cytoskeleton.²⁹ Phalloidin is a cyclic peptide produced by *Amanita phalloides* that can bind to and stabilize F-actin.³⁰ FITC fluorescent substance-labeled phalloidins can specifically bind to F-actin in eukaryotic cells, thus indicating the distribution of microfilaments in the cytoskeleton of cells.³¹ Thus, we analyzed the ITGB4, FLNA, PLEC,

ITGA3 and phalloidin in TCN1 knockdown and TCN1-overexpression cells using immunofluorescence staining. In TCN1-KDC cells, the fluorescence signals of ITGB4, PLEC, ITGA3 and phalloidin were clustered and completely colocalized (Fig. 4A, Supplementary Fig. 3A-H). In TCN1-KD1 and TCN1-KD2 cells, the fluorescence signal of ITGB4 was weak, while PLEC and phalloidin exhibited a diffuse filamentous distribution. However, the fluorescence signals of ITGB4, PLEC, ITGA3 and phalloidin in TCN1-OE cells were stronger than those in TCN1-OEC cells. Our results showed that ITGB4, PLEC, and phalloidin are also expressed in human normal colonic epithelial cells (Supplementary Fig. 3M). FLNA can bind F-actin filaments to form a stable cytoskeleton.³² TCN1 knockdown also decreased the level of FLNA in HCT116 cells (Fig. 4B). Immunofluorescence staining showed that FLNA signal almost disappeared in TCN1 knockdown cells, indicating

that TCN1 may regulate the stability of FLNA. However, the fluorescence signal of FLNA in TCN1-OE cells was stronger than that in TCN1-OEC cells. These results suggest that the degradation of ITGB4 induced by TCN1 inactivation may directly lead to the structural damage of hemidesmosomes and affects cytoskeletal reconstruction.

Transmission electron microscope analysis showed that actin filaments were cross-linked in the cytoplasm, and a dense network structure in the cytoplasm and basal layer of control cells (Fig. 4C). These three-dimensional structures have high strength and can support the extension of pseudopodia. In TCN1-knockdown cells, the three-dimensional network structure of actin filaments is destroyed, resulting in the formation of long and straight filaments. These parallel microfilaments can affect the formation of pseudopodia and lead to the destruction of the cytoskeleton.³¹ The results demonstrated that TCN1-knockdown

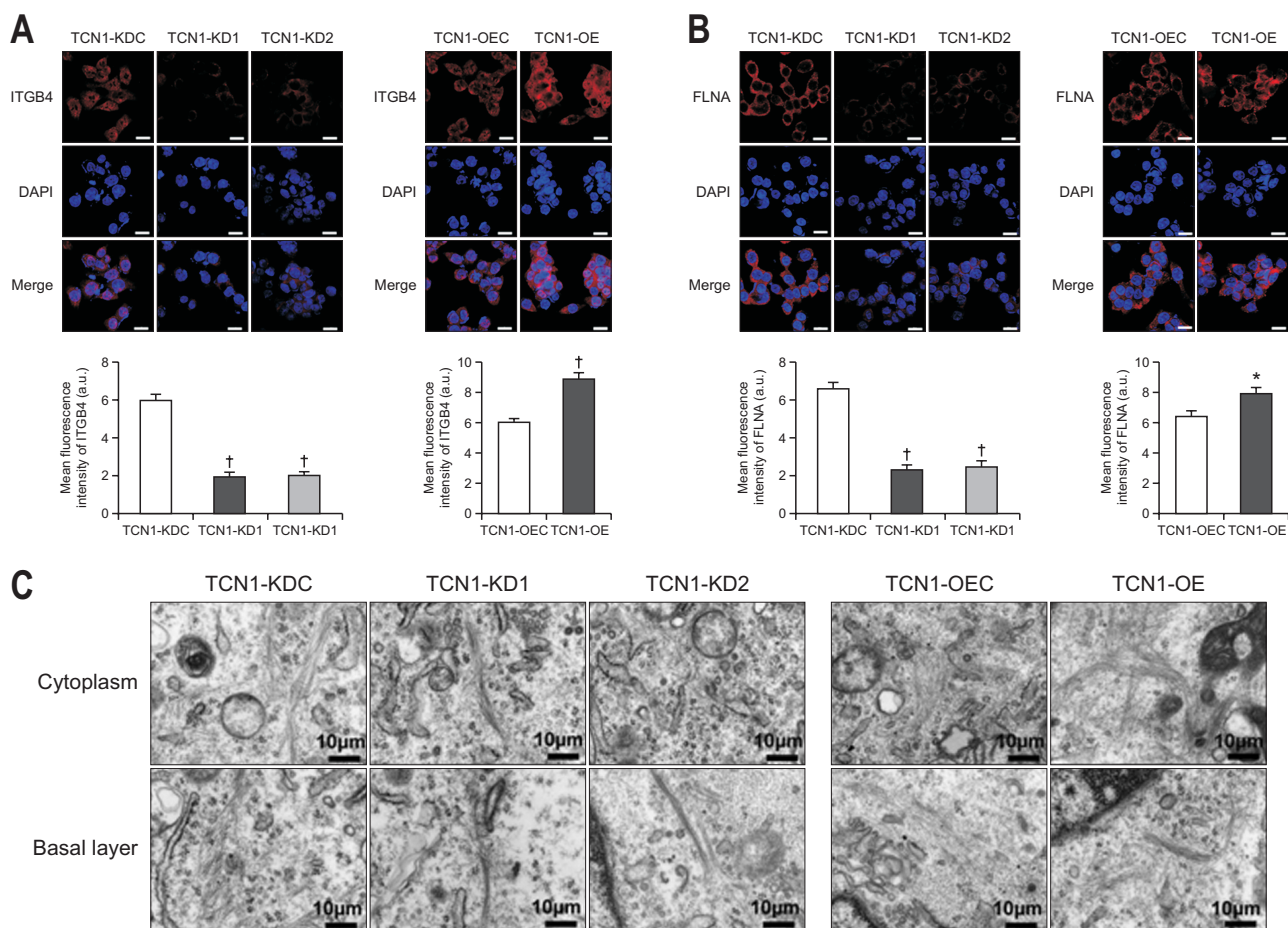


Fig. 4. Transcobalamin 1 (TCN1) deficiency causes cytoskeletal network damage. (A) Representative images and quantification of integrin subunit $\beta 4$ (ITGB4) in TCN1-KD and TCN1-OE HCT116 cells detected by immunofluorescence staining ($n=6$). (B) Representative images and quantification of filamin A (FLNA) in TCN1-KD and TCN1-OE HCT116 cells detected by immunofluorescence staining ($n=6$). Scale bars=100 μm . The nuclei were stained with DAPI. (C) Representative images of the microfilament network structure in TCN1-KD and TCN1-OE HCT116 cells detected by transmission electron microscopy ($n=6$). Scale bars=10 μm . All experimental data are presented as the mean \pm SD.

TCN1-KD, TCN1-knockdown, TCN1-OE, TCN1-overexpression; a.u., absorbance unit. Statistical significance: * $p<0.05$, † $p<0.01$.

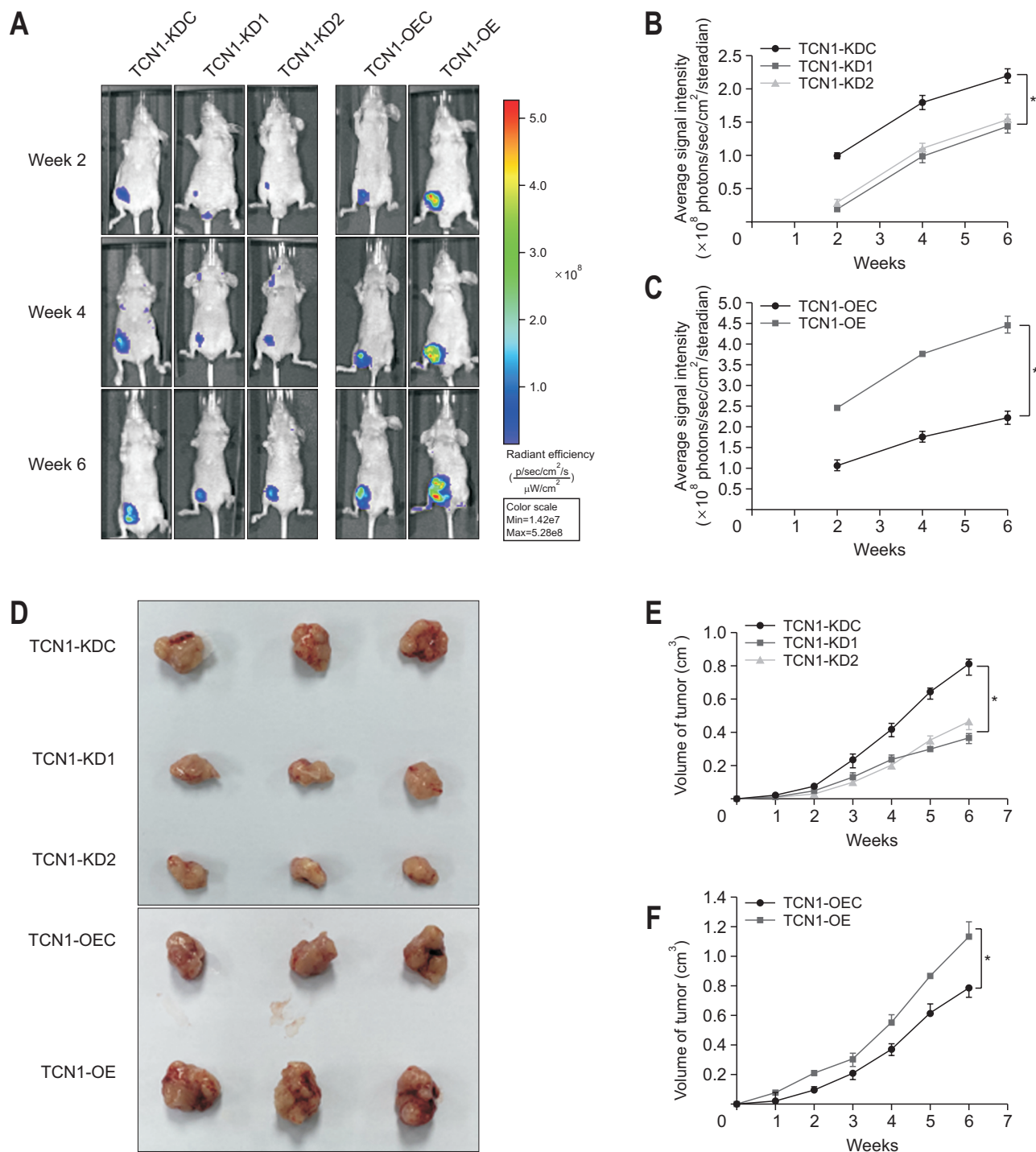


Fig. 5. Transcobalamin 1 (TCN1) deficiency inhibits tumorigenesis in a colorectal cancer xenograft model. (A) Representative bioluminescent images of tumors in nude mice are shown. (B, C) The photon flux in the bioluminescent images of tumors was quantified (n=6). (D) The tumors from each mouse were excised and photographed. (E, F) The tumor volume was calculated using the formula $0.5 \times \text{length} \times \text{width}^2$ (n=6). (G) The expression of TCN1 and integrin subunit $\beta 4$ (ITGB4) in tumor tissues was assessed by quantitative polymerase chain reaction. (H) The expression of TCN1 and ITGB4 in tumor tissues was assessed by Western blot analysis. GAPDH served as the loading control. (I-K) The Ki-67 and proliferating cell nuclear antigen (PCNA) expression levels in xenograft tumors were immunohistochemically evaluated. All experimental data are presented as the mean \pm SD.

TCN1-KD, TCN1-knockdown, TCN1-OE, TCN1-overexpression. *Statistical significance: $p < 0.01$.

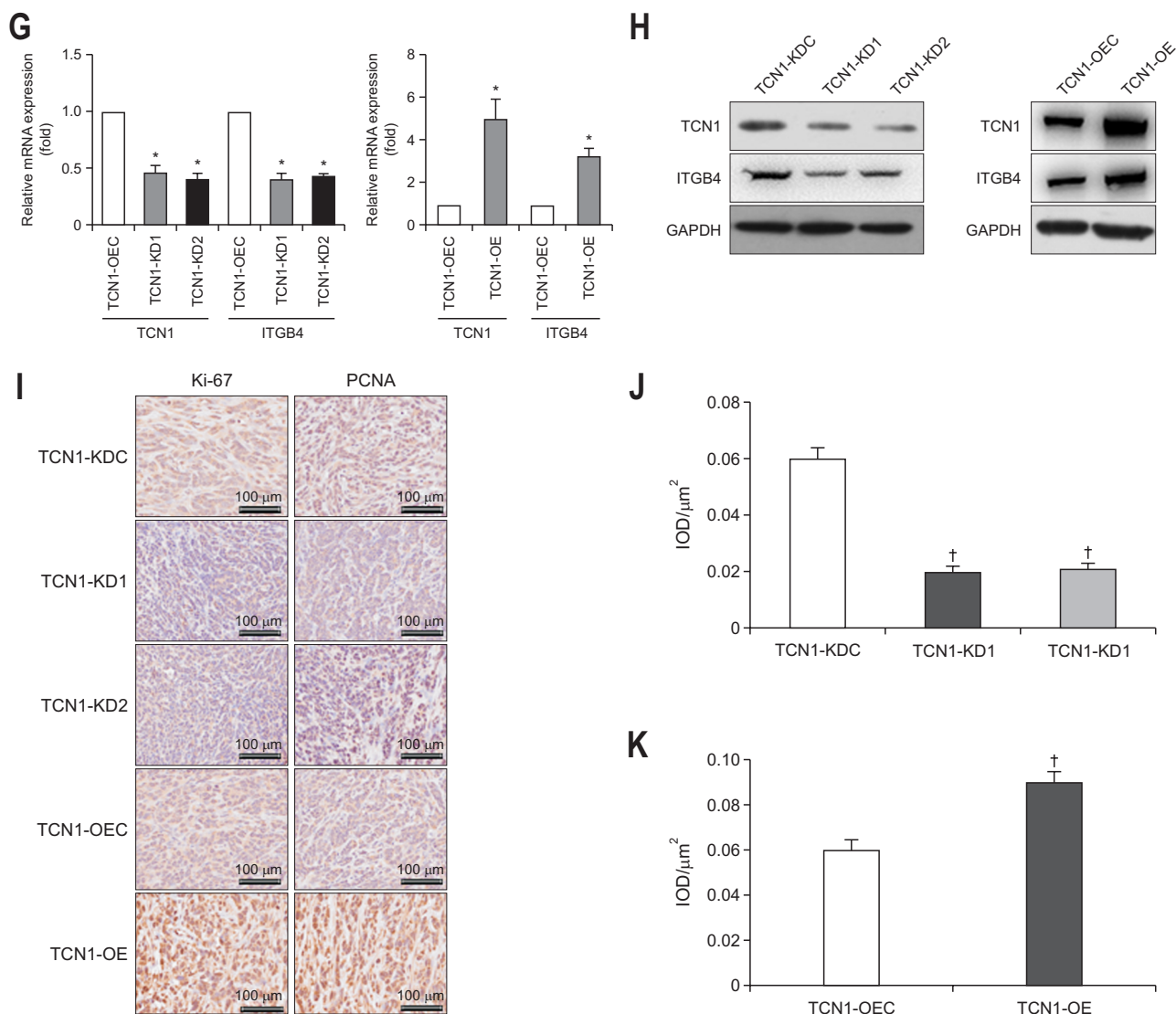


Fig. 5. Continued.

may cause damage to the cytoskeletal network by regulating ITGB4 signaling.

5. Inactivation of TCN1 inhibits tumorigenesis in a CRC xenograft model

We established a nude mouse subcutaneous xenograft model using TCN1-KDC, TCN1-OEC, TCN1-KD, TCN1-KD2, and TCN1-OE cells to further evaluate the *in vivo* tumorigenic effect of TCN1-knockdown and TCN1-overexpressing cells (Fig. 5). Consistent with the *in vitro* results, bioluminescence imaging showed TCN1-knockdown cells produced a significant decrease in the tumor size compared with TCN1-KDC group ($p < 0.01$) (Fig. 5B), and TCN1-overexpression cells produced a marked increase in the tumor size compared with the TCN1-OEC group ($p < 0.01$) (Fig. 5C). Meanwhile, the tumor volume was

more markedly decreased in the TCN1-KD and TCN1-KD2 groups than in the TCN1-KDC group ($p < 0.01$) (Fig. 5D and E). The tumor volume in the TCN1-OE group was substantially increased compared with the TCN1-OEC group ($p < 0.01$) (Fig. 5D and F). The TCN1 and ITGB4 expression levels in xenograft tumors were evaluated using Q-PCR and Western blot. TCN1 and ITGB4 expression was more markedly decreased in the TCN1-KD1 and TCN1-KD2 groups than in the TCN1-KDC group ($p < 0.01$) and was substantially increased in TCN1-OE cells compared with TCN1-OEC cells ($p < 0.01$) (Fig. 5G and H). The expression levels of the proliferation-related proteins Ki-67 and proliferating cell nuclear antigen (PCNA) in xenograft tumors were immunohistochemically evaluated (Fig. 5I-K). Ki-67 and PCNA expression decreased more drastically in the TCN1-KD1 and TCN1-KD2 groups than in the

TCN1-KDC group ($p < 0.01$) (Fig. 5I-K) and was increased in the TCN1-OE group compared with the TCN1-OEC group ($p < 0.01$) (Fig. 5I-K). The results were similar to the *in vitro* results and further revealed that TCN1 knockdown inhibit tumorigenesis *in vivo*, indicating TCN1 knock-down synergized with ITGB4-induced inactivation of Ki-67 and PCNA in CRC cells.

6. TCN1 deficiency inhibits metastatic engraftment in the peritoneum *in vivo*

Since TCN1 deficiency impairs the adhesion and growth of CRC cells, we assessed the effect of TCN1 knockdown and TCN1 overexpression on the metastasis ability of HCT116 cells *in vivo* (Fig. 6). Bioluminescence imaging showed that most of the metastatic foci were found in the peritoneal cavity in mice ($p < 0.01$) (Fig. 6A and B). The TCN1-KD1 and TCN1-KD2 groups had few

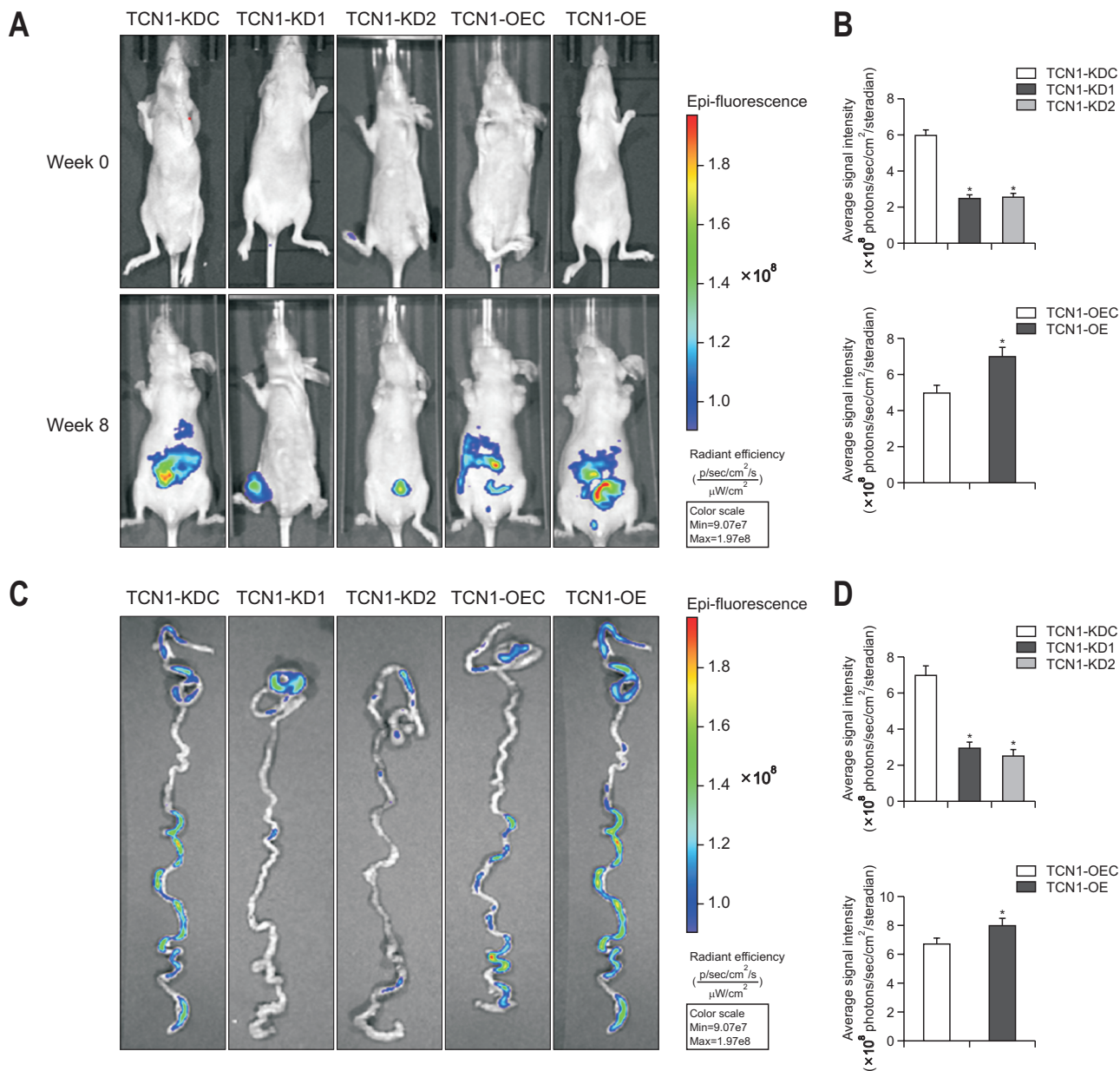


Fig. 6. Transcobalamin 1 (TCN1) deficiency inhibited metastatic engraftment in the peritoneum *in vivo*. (A, B) Representative bioluminescent images and quantification of metastatic foci in nude mice after 8 weeks are shown, $n=6$. (C, D) Bioluminescent images and quantification of metastatic foci in the intestines of nude mice after 8 weeks are shown ($n=6$). (E-G) Immunohistochemical analysis of TCN1 and integrin subunit B4 (ITGB4) expression in metastatic tumor foci. Representative pictures of immunohistochemical staining are shown ($n=6$). Scale bars=100 μ m. All experimental data are presented as the mean \pm SD.

TCN1-KD, TCN1-knockdown, TCN1-OE, TCN1-overexpression. *Statistical significance: $p < 0.01$.

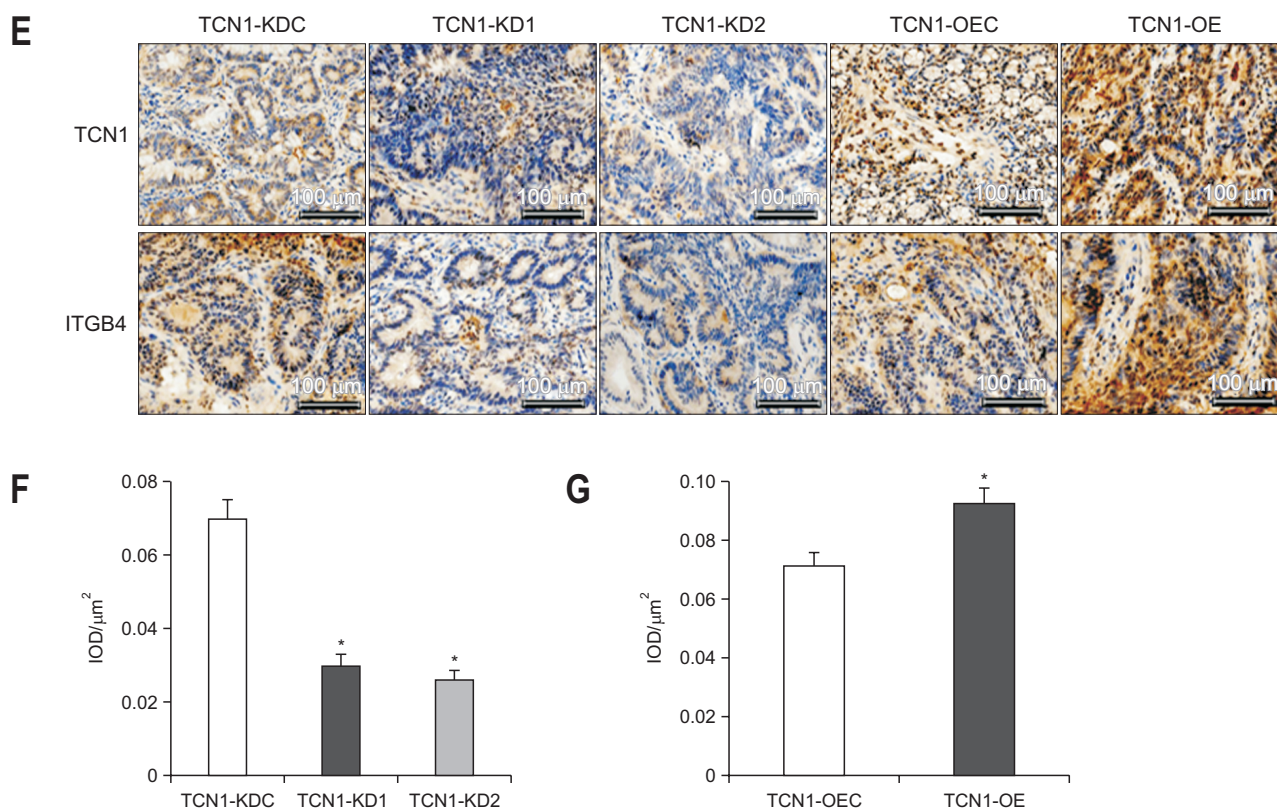


Fig. 6. Continued.

tumor nodules. The area of metastatic foci was decreased more in the TCN1-KD1 and TCN1-KD2 groups than in the TCN1-KDC group and was increased in the TCN1-OE group compared with the TCN1-OEC group ($p < 0.01$) (Fig. 6C and D). TCN1 and ITGB4 expression was detected in metastatic foci in the peritoneal cavity using immunohistochemistry (Fig. 6E). TCN1 and ITGB4 expression was decreased more in the TCN1-KD1 and TCN1-KD2 groups than in the TCN1-KDC group, and was increased in the TCN1-OE group compared with the TCN1-OEC group ($p < 0.01$) (Fig. 6F and G). These results suggest that TCN1 deficiency inhibits the metastasis and implantation of CRC cells *in vivo* after intravenous injection.

DISCUSSION

CRC is a pathological tumor in the colon or rectum, which may invade and spread to distant organs.³³ Most CRC patients are elderly or have an unhealthy lifestyle, and only a small number of cases are caused by genetic diseases.^{34,35} Despite significant progress in surgery and treatment, the long-term survival rate is still unsatisfactory, mainly because CRC is often diagnosed at an advanced stage.^{36,37} At present, the diagnosis, recurrence, and metas-

tasis of CRC mainly rely on colonoscopy and other imaging examinations, which are often delayed. Therefore, it is urgent to find new sensitive biomarkers to ensure early diagnosis and timely treatment of CRC, and even predict the occurrence of CRC.

Increasing evidence has shown that TCN1 is highly expressed in metastatic epithelial tumors such as breast cancer, thyroid cancer, laryngeal cancer, and cervical cancer.^{8,10,11,13,38} Bioinformatics analysis and meta-data analysis based on the colon and rectal adenocarcinomas database showed that TCN1 was overexpressed as an oncogene in CRC.¹⁴ The next-generation sequencing results showed that TCN1 was the second most upregulated mRNA in CRC.¹⁵ The results provide more evidence for the role of TCN1 in colon carcinogenesis, suggesting that TCN1 may be a potential new gene biomarker. Our study found that the high expression of TCN1 and ITGB4 is positively correlated with the poor prognosis of CRC, suggesting that TCN1 may positively regulate the expression of ITGB4 and promote the development of CRC, and TCN1-knockdown promoted the apoptosis of CRC cells and inhibited the proliferation and invasion of CRC cells.

Although it has been reported that TCN1 regulates malignant cell metastasis and glycolysis,^{10,11,13} the mechanism by which TCN1 promotes tumor development is still un-

clear. To reveal the potential mechanism of TCN1 in CRC, we selected genes related to TCN1 to determine its mode of action. TCN1 has the role of an oncogene,¹⁴ so we selected genes positively related to TCN1 for Gene Ontology and GSEA. The results showed that TCN1 was related to the Wnt signaling pathway, Notch signaling pathway, and tumor-related genes involved in cell division, migration, or proliferation. More importantly, our results showed that TCN1 interacts directly with the ITGB4 promoter, which complements our understanding of the relationship between TCN1 and integrins. TCN1 deficiency can down-regulate ITGB4 signaling and cause damage to the cytoskeletal network. The evidence suggests that TCN1 affects tumorigenesis at least partly by regulating the expression of ITGB4, while overexpression of ITGB4 upregulate the Notch signaling pathway.³⁹ According to these results, we speculate that integrins, including ITGB4, may be TCN1 receptors on the cell membrane that can promote cell signal transduction. Moreover, through the analysis of patient samples and clinical data, we found that the expression level of ITGB4 was upregulated in CRC tissues, which was associated with poor prognosis of CRC and was positively correlated with TCN1.

Integrins are also the main adhesion molecules connecting the ECM and cytoskeleton.⁴⁰ Cytoskeleton is a network of microfilaments, interfilaments and microtubules. Actin cytoskeleton remodeling plays an important role in tumor cell migration and invasion.⁴¹ It was reported that ITGB4 interacts with the ECM and cytoskeleton and plays an important role in many physiological processes such as cell proliferation, carcinogenesis, and immune response.^{42,43} ITGB4 has a long cytoplasmic domain and unique cytoskeleton and signal function.⁴⁴ ITGB4 is related to the actin cytoskeleton, and its basic function in polarized epithelial cells is to form stable cell attachment by forming hemidesmosomes and basement membrane. The main structure of hemidesmosomes is composed of PLEC and ITGB4.⁴⁵ Under normal physiological conditions, TCN1 may bind to the ITGB4-*PLEC* complex to maintain the three-dimensional filamentous structure of hemidesmosomes. Our results first showed that TCN1 interacted directly with ITGB4 and then regulated ITGB4 and *FLNA* expression to affect the F-actin cytoskeleton. The decrease in ITGB4 protein levels led to the degradation of the ITGB4-*PLEC* complex. In addition, the decrease in *FLNA* prevented F-actin from forming vertical branches. These factors lead to the destruction of three-dimensional structure of cytoskeleton microfilaments and cytoskeleton network structure.⁴⁶

Metastasis is a complex biological cascade in which tumor cells invade the local environment, migrate to distant tissues, and finally colonize.^{47,48} Upregulation of ITGB4

expression is positively correlated with CRC progression⁴⁹ and promotes EMT in prostate cancer.⁵⁰ EMT promotes tumor metastasis by promoting the invasion of epithelial malignant cells.⁵¹ In the process of EMT, cells lose adhesion properties and undergo polarity changes accompanied by the reorganization of the cytoskeleton and the upregulation of ECM components, which eventually facilitate migration and invasion.⁵² Therefore, inhibiting the occurrence of EMT has become a research hotspot in the treatment of CRC metastasis. GSEA showed that ITGB4 was significantly involved in the focal adhesion signaling pathway.⁵³ The overexpression of ITGB4 was significantly correlated with the upregulation of focal adhesion-associated genes.³⁹ Focal adhesion and metastasis are the key to cell migration and invasion.⁵⁴ Focal adhesion signaling pathway plays an important role in EMT of prostate cancer,⁵⁵ and ITGB4 mediates the activation of the focal adhesion signaling pathway in ovarian cancer⁵⁶ and hepatocellular carcinoma.⁵⁷ In addition, it has been reported that ITGB4 and the focal adhesion signaling pathway are involved in the development of CRC.^{58,59} Similarly, our study showed that TCN1 inhibited the expression of *FLNA*, F-actin, and *PLEC* by inhibiting the ITGB4 pathway.

Only cells with adhesion, migration, invasion, and proliferation abilities can form new tumor lesions,⁵³ and ITGB4 mediates the invasion and migration of gastric cancer cells.⁶⁰ The results showed that TCN1 interacts with ITGB4, and the level of ITGB4 decreased significantly in TCN1-deficient cells. Therefore, this effect will lead to the decrease of adhesion, survival, and proliferation of TCN1-knockdown cells.⁵⁹ Naturally, circulating tumor cells in the blood may lose the ability to adhere to the vascular endothelium and thus lose the ability to migrate into new tissues and eventually form metastatic colonies. These results provide a new idea for targeting the TCN1/ITGB4 signaling pathway in the treatment of CRC metastasis, but further research is still needed.

In conclusion, our data revealed that TCN1 was significantly overexpressed in CRC tissues and correlated with the pathological features of advanced CRC. TCN1 deficiency causes cytoskeletal network damage, and inhibits cell division, cell migration, and proliferation by regulating ITGB4 signal pathway. Collectively, TCN1 might be a therapeutic target and prognostic marker for the individualized treatment of CRC.

CONFLICTS OF INTEREST

No potential conflict of interest relevant to this article was reported.

ACKNOWLEDGEMENTS

This work was supported by Suqian Science and Technology Innovation Special Project (number: S201913).

AUTHOR CONTRIBUTIONS

Study concept and design: X.Z., C.X. Data acquisition: X.J., H.H. Data analysis and interpretation: Q.Z., X.S. Drafting of the manuscript: X.Z., D.H. Critical revision of the manuscript for important intellectual content: C.X. Statistical analysis: X.Z., D.H. Obtained funding: X.Z. Administrative, technical, or material support: X.Z., C.X. Study supervision: C.X. Approval of final manuscript: all authors.

ORCID

Xinqiang Zhu	https://orcid.org/0000-0002-7674-8555
Xuetong Jiang	https://orcid.org/0000-0002-7591-3459
Qinglin Zhang	https://orcid.org/0000-0003-3942-7469
Hailong Huang	https://orcid.org/0000-0001-8401-4845
Xiaohong Shi	https://orcid.org/0000-0003-0557-1980
Daorong Hou	https://orcid.org/0000-0002-7755-9326
Chungen Xing	https://orcid.org/0000-0001-7865-1258

SUPPLEMENTARY MATERIALS

Supplementary materials can be accessed at <https://doi.org/10.5009/gnl210494>.

REFERENCES

1. Siegel RL, Miller KD, Jemal A. Cancer statistics, 2018. *CA Cancer J Clin* 2018;68:7-30.
2. Kawaguchi N, Tashiro K, Taniguchi K, et al. Nogo-B (Reticulon-4B) functions as a negative regulator of the apoptotic pathway through the interaction with c-FLIP in colorectal cancer cells. *Biochim Biophys Acta Mol Basis Dis* 2018;1864:2600-2609.
3. Bray F, Ferlay J, Soerjomataram I, Siegel RL, Torre LA, Jemal A. Global cancer statistics 2018: GLOBOCAN estimates of incidence and mortality worldwide for 36 cancers in 185 countries. *CA Cancer J Clin* 2018;68:394-424.
4. Chen W, Zheng R, Baade PD, et al. Cancer statistics in China, 2015. *CA Cancer J Clin* 2016;66:115-132.
5. Lee TY, Liu CL, Chang YC, et al. Increased chemoresistance via Snail-Raf kinase inhibitor protein signaling in colorectal cancer in response to a nicotine derivative. *Oncotarget* 2016;7:23512-23520.
6. Deng WW, Hu Q, Liu ZR, et al. KDM4B promotes DNA damage response via STAT3 signaling and is a target of CREB in colorectal cancer cells. *Mol Cell Biochem* 2018;449:81-90.
7. Wang Y, Yue C, Fang J, et al. Transcobalamin I: a novel prognostic biomarker of neoadjuvant chemotherapy in locally advanced hypopharyngeal squamous cell cancers. *Onco Targets Ther* 2018;11:4253-4261.
8. Chong LY, Cheok PY, Tan WJ, et al. Keratin 15, transcobalamin I and homeobox gene Hox-B13 expression in breast phyllodes tumors: novel markers in biological classification. *Breast Cancer Res Treat* 2012;132:143-151.
9. Allen LH, Miller JW, de Groot L, et al. Biomarkers of Nutrition for Development (BOND): vitamin B-12 review. *J Nutr* 2018;148(suppl_4):1995S-2027S.
10. Waibel R, Treichler H, Schaefer NG, et al. New derivatives of vitamin B12 show preferential targeting of tumors. *Cancer Res* 2008;68:2904-2911.
11. Lyon P, Strippoli V, Fang B, Cimmino L. B vitamins and one-carbon metabolism: implications in human health and disease. *Nutrients* 2020;12:2867.
12. Martinelli M, Scapoli L, Mattei G, et al. A candidate gene study of one-carbon metabolism pathway genes and colorectal cancer risk. *Br J Nutr* 2013;109:984-989.
13. Lederer AK, Hannibal L, Hettich M, et al. Vitamin B12 status upon short-term intervention with a vegan diet: a randomized controlled trial in healthy participants. *Nutrients* 2019;11:2815.
14. Chu CM, Yao CT, Chang YT, et al. Gene expression profiling of colorectal tumors and normal mucosa by microarrays meta-analysis using prediction analysis of microarray, artificial neural network, classification, and regression trees. *Dis Markers* 2014;2014:634123.
15. Li M, Zhao LM, Li SL, et al. Differentially expressed lncRNAs and mRNAs identified by NGS analysis in colorectal cancer patients. *Cancer Med* 2018;7:4650-4664.
16. Zhu X, Yi K, Hou D, et al. Clinicopathological analysis and prognostic assessment of transcobalamin I (TCN1) in patients with colorectal tumors. *Med Sci Monit* 2020;26:e923828.
17. Liu GJ, Wang YJ, Yue M, et al. High expression of TCN1 is a negative prognostic biomarker and can predict neoadjuvant chemosensitivity of colon cancer. *Sci Rep* 2020;10:11951.
18. Giancotti FG. Targeting integrin beta4 for cancer and anti-angiogenic therapy. *Trends Pharmacol Sci* 2007;28:506-511.
19. Wang L, Zhang X, Pang N, et al. Glycation of vitronectin inhibits VEGF-induced angiogenesis by uncoupling VEGF receptor-2- $\alpha v\beta 3$ integrin cross-talk. *Cell Death Dis*

- 2015;6:e1796.
20. Xiao T, Takagi J, Collier BS, Wang JH, Springer TA. Structural basis for allostery in integrins and binding to fibrinogen-mimetic therapeutics. *Nature* 2004;432:59-67.
 21. Nagata M, Noman AA, Suzuki K, et al. ITGA3 and ITGB4 expression biomarkers estimate the risks of locoregional and hematogenous dissemination of oral squamous cell carcinoma. *BMC Cancer* 2013;13:410.
 22. Wang H, Rana S, Giese N, Büchler MW, Zöller M. Tspan8, CD44v6 and alpha6beta4 are biomarkers of migrating pancreatic cancer-initiating cells. *Int J Cancer* 2013;133:416-426.
 23. Zhang W, Zhang B, Vu T, et al. Molecular characterization of pro-metastatic functions of β 4-integrin in colorectal cancer. *Oncotarget* 2017;8:92333-92345.
 24. Zhong F, Lu HP, Chen G, et al. The clinical significance and potential molecular mechanism of integrin subunit beta 4 in laryngeal squamous cell carcinoma. *Pathol Res Pract* 2020;216:152785.
 25. Blackhall FH, Peters S, Bubendorf L, et al. Prevalence and clinical outcomes for patients with ALK-positive resected stage I to III adenocarcinoma: results from the European Thoracic Oncology Platform Lungscape Project. *J Clin Oncol* 2014;32:2780-2787.
 26. Colla S, Tagliaferri S, Morandi F, et al. The new tumor-suppressor gene inhibitor of growth family member 4 (ING4) regulates the production of proangiogenic molecules by myeloma cells and suppresses hypoxia-inducible factor-1 alpha (HIF-1alpha) activity: involvement in myeloma-induced angiogenesis. *Blood* 2007;110:4464-4475.
 27. Yang N, Gong F, Sun L, et al. Poly (ADP-ribose) polymerase-1 binds to BCL2 major breakpoint region and regulates BCL2 expression. *J Cell Biochem* 2010;110:1208-1218.
 28. Wu D, Xu Y, Ding T, Zu Y, Yang C, Yu L. Pairing of integrins with ECM proteins determines migrasome formation. *Cell Res* 2017;27:1397-1400.
 29. Litjens SH, Koster J, Kuikman I, van Wilpe S, de Pereda JM, Sonnenberg A. Specificity of binding of the plectin actin-binding domain to beta4 integrin. *Mol Biol Cell* 2003;14:4039-4050.
 30. Pospich S, Merino F, Raunser S. Structural effects and functional implications of phalloidin and jasplakinolide binding to actin filaments. *Structure* 2020;28:437-449.
 31. Hong D, Zhang X, Li R, et al. Deletion of TMEM268 inhibits growth of gastric cancer cells by downregulating the ITGB4 signaling pathway. *Cell Death Differ* 2019;26:1453-1466.
 32. Wang W, Zuidema A, Te Molder L, et al. Hemidesmosomes modulate force generation via focal adhesions. *J Cell Biol* 2020;219:e201904137.
 33. Weinberg BA, Marshall JL, Salem ME. The growing challenge of young adults with colorectal cancer. *Oncology (Williston Park)* 2017;31:381-389.
 34. O'Keefe SJ. Diet, microorganisms and their metabolites, and colon cancer. *Nat Rev Gastroenterol Hepatol* 2016;13:691-706.
 35. Durinikova E, Buzo K, Arena S. Preclinical models as patients' avatars for precision medicine in colorectal cancer: past and future challenges. *J Exp Clin Cancer Res* 2021;40:185.
 36. Heinemann V, von Weikersthal LF, Decker T, et al. FOLFIRI plus cetuximab versus FOLFIRI plus bevacizumab as first-line treatment for patients with metastatic colorectal cancer (FIRE-3): a randomised, open-label, phase 3 trial. *Lancet Oncol* 2014;15:1065-1075.
 37. Boyle T, Fritschi L, Platell C, Heyworth J. Lifestyle factors associated with survival after colorectal cancer diagnosis. *Br J Cancer* 2013;109:814-822.
 38. Abdulrahman SS, Mohammad DN, Hamied MA, Abdulqadir MO. Immunohistochemical evaluation of salivary gland tumors differentiation and proliferation by using calponin and telomerase. *Saudi Dent J* 2019;31:105-114.
 39. Zhuang H, Zhou Z, Ma Z, et al. Characterization of the prognostic and oncologic values of ITGB superfamily members in pancreatic cancer. *J Cell Mol Med* 2020;24:13481-13493.
 40. Woo JA, Zhao X, Khan H, et al. Slingshot-Cofilin activation mediates mitochondrial and synaptic dysfunction via A β ligation to β 1-integrin conformers. *Cell Death Differ* 2015;22:921-934.
 41. Padilla-Rodriguez M, Parker SS, Adams DG, et al. The actin cytoskeletal architecture of estrogen receptor positive breast cancer cells suppresses invasion. *Nat Commun* 2018;9:2980.
 42. Bianconi D, Unseld M, Prager GW. Integrins in the spotlight of cancer. *Int J Mol Sci* 2016;17:2037.
 43. Ginsberg MH. Integrin activation. *BMB Rep* 2014;47:655-659.
 44. Li J, Luo M, Ou H, Liu X, Kang X, Yin W. Integrin β 4 promotes invasion and anoikis resistance of papillary thyroid carcinoma and is consistently overexpressed in lymphovascular tumor thrombus. *J Cancer* 2019;10:6635-6648.
 45. Kadeer A, Maruyama T, Kajita M, et al. Plectin is a novel regulator for apical extrusion of RasV12-transformed cells. *Sci Rep* 2017;7:44328.
 46. Bouameur JE, Favre B, Fontao L, Lingasamy P, Bègré N, Borradori L. Interaction of plectin with keratins 5 and 14: dependence on several plectin domains and keratin quaternary structure. *J Invest Dermatol* 2014;134:2776-2783.
 47. Ganguly KK, Pal S, Moulik S, Chatterjee A. Integrins and metastasis. *Cell Adh Migr* 2013;7:251-261.
 48. Yoshioka T, Otero J, Chen Y, et al. β 4 Integrin signaling induces expansion of prostate tumor progenitors. *J Clin Invest* 2013;123:682-699.
 49. Kröger C, Afeyan A, Mraz J, et al. Acquisition of a hybrid E/

- M state is essential for tumorigenicity of basal breast cancer cells. *Proc Natl Acad Sci U S A* 2019;116:7353-7362.
50. Masugi Y, Yamazaki K, Emoto K, et al. Upregulation of integrin $\beta 4$ promotes epithelial-mesenchymal transition and is a novel prognostic marker in pancreatic ductal adenocarcinoma. *Lab Invest* 2015;95:308-319.
 51. Yao B, Li Y, Wang L, et al. MicroRNA-3194-3p inhibits metastasis and epithelial-mesenchymal transition of hepatocellular carcinoma by decreasing Wnt/ β -catenin signaling through targeting BCL9. *Artif Cells Nanomed Biotechnol* 2019;47:3885-3895.
 52. Scheau C, Badarau IA, Costache R, et al. The role of matrix metalloproteinases in the epithelial-mesenchymal transition of hepatocellular carcinoma. *Anal Cell Pathol (Amst)* 2019;2019:9423907.
 53. Gan L, Meng J, Xu M, et al. Extracellular matrix protein 1 promotes cell metastasis and glucose metabolism by inducing integrin $\beta 4$ /FAK/SOX2/HIF-1 α signaling pathway in gastric cancer. *Oncogene* 2018;37:744-755.
 54. Kurenova E, Liao J, He DH, et al. The FAK scaffold inhibitor C4 disrupts FAK-VEGFR-3 signaling and inhibits pancreatic cancer growth. *Oncotarget* 2013;4:1632-1646.
 55. Ning Z, Wang A, Liang J, et al. USP22 promotes epithelial-mesenchymal transition via the FAK pathway in pancreatic cancer cells. *Oncol Rep* 2014;32:1451-1458.
 56. Wu A, Zhang S, Liu J, et al. Integrated analysis of prognostic and immune associated integrin family in ovarian cancer. *Front Genet* 2020;11:705.
 57. Li J, Hao N, Han J, Zhang M, Li X, Yang N. ZKSCAN3 drives tumor metastasis via integrin $\beta 4$ /FAK/AKT mediated epithelial-mesenchymal transition in hepatocellular carcinoma. *Cancer Cell Int* 2020;20:216.
 58. Tai YL, Lai IR, Peng YJ, Ding ST, Shen TL. Activation of focal adhesion kinase through an interaction with $\beta 4$ integrin contributes to tumorigenicity of colon cancer. *FEBS Lett* 2016;590:1826-1837.
 59. Jang B, Jung H, Choi S, Lee YH, Lee ST, Oh ES. Syndecan-2 cytoplasmic domain up-regulates matrix metalloproteinase-7 expression via the protein kinase C γ -mediated FAK/ERK signaling pathway in colon cancer. *J Biol Chem* 2017;292:16321-16332.
 60. Yang ZY, Jiang H, Qu Y, et al. Metalloproteinase-1 regulates invasion and migration of gastric cancer cells partially through integrin $\beta 4$. *Carcinogenesis* 2013;34:2851-2860.